Bulletin of the Seismological Society of America, Vol. 109, No. 6, pp. 2764–2766, December 2019, doi: 10.1785/0120190122

Reply to "Comment on 'Interpretation of Kappa and f_{max} Filters as Source Effect' by Igor A. Beresnev" by Arthur Frankel

by Igor A. Beresnev

I agree with the statement of Frankel (2019) that the path attenuation is a factor affecting the shape of the high-frequency spectrum in the far field. Beresnev (2019, p. 822) is explicit in acknowledging that the observed steep high-frequency fall-off "is in addition to the decay produced by regular anelastic attenuation along the propagation path." The term source spectra is used throughout the article of Beresnev (2019) to emphasize that the discussion was centered upon the source effect. The regular site and path contributions apply as usual.

I also previously directly addressed the effect of rupture complexity on the shape of the seismic spectra in the near field (Beresnev, 2017). The analysis was performed via the direct computation of the representation integral of elasticity. Specifically, randomly disturbing the total slip and the maximum slip rate over the fault plane or introducing asperities did not lead to any appreciable differences in the shape of the radiated Fourier spectra. It was argued that the functional form of the source time function was the predominant factor in forming the spectra, although Beresnev (2019, pp. 822 and 825) repeatedly mentioned that the spectral slope could be disturbed by the directivity, path, and site effects.

The near-field frequency spectrum can be obtained by taking the Fourier transform of the representation integral. For a source time function in the form of a radially propagating rupture

$$\Delta u(\boldsymbol{\xi}, t) = U(\boldsymbol{\xi})\Delta u(t - r/v), \tag{1}$$

in which $U(\boldsymbol{\xi})$ is the distribution of final-slip values over the fault plane, r is the distance from hypocenter, and v is the rupture-propagation speed, the Fourier spectrum of the seismic displacement at the observation point $\mathbf{x}$ is

$$\mathbf{u}(\mathbf{x}, \omega) = \Delta u(\omega) \iint U(\boldsymbol{\xi}) F(\mathbf{x}, \boldsymbol{\xi}, r, \omega) d\Sigma(\boldsymbol{\xi}) \tag{2}$$

(Beresnev, 2017, his equation 4). Here, $\Delta u(\omega)$ is the Fourier transform of the source time function and $F(\mathbf{x}, \boldsymbol{\xi}, r, \omega)$ is a function of complicated form. The integration is carried out over the fault plane and a homogeneous space with given elastic constants is assumed. The spectrum of radiation is thus the one of the source time function, modulated by the integral representing the finite-fault spatial directivity. Equation (2) underscores the universal controlling effect of $\Delta u(\omega)$ over the spectral content of radiation.

As Frankel (2019) mentions, a classic example of the effect of source finiteness on the radiated spectrum is a unidirectional rupture propagation with constant velocity. In the limits of (1) a near-line source with small width W, extending to the length L along the coordinate ξ_1; (2) small source dimensions; and (3) the far field, for the rupture propagating along ξ_1, the modulus of equation (2) reduces to

$$|\mathbf{u}(\mathbf{x}, \omega)| = \omega W |\Delta u(\omega)||\mathrm{I}(\mathbf{x}, \omega)|, \tag{3}$$

in which

$$\mathrm{I}(\mathbf{x}, \omega) = \int_0^L \exp\left[i\omega \left(\frac{\xi_1}{v} - \frac{\xi_1 \cos \Psi}{c} \right) \right] d\xi_1, \tag{4}$$

in which c is either the P- or S-wave propagation speed, and Ψ is the angle between the direction to the receiver and the axis ξ_1 (Aki and Richards, 1980, their equation 14.18). The quantity $|\mathrm{I}(\mathbf{x}, \omega)|$ is the directivity spectrum modifying that of the source time function owing to the source finiteness. For constant v, $|\mathrm{I}(\mathbf{x}, \omega)|$ evaluates to

$$|\mathrm{I}(\mathbf{x}, \omega)| = L \left| \frac{\sin X}{X} \right|, \tag{5}$$

in which $X = (\omega L/2)[1/v - (\cos \Psi)/c]$ (ibid.). It follows, as Frankel (2019) correctly points out, that the effect of constant rupture speed results in the multiplication of the underlying spectrum of the source time function by that of the sinc function, producing a high-frequency fall-off that is steeper by the additional factor of ω^{-1} (Aki and Richards, 1980, their fig. 14.3 and p. 810). However, it is worth asking the question whether the same effect will hold for a variable rupture velocity.

The directivity spectral modifier $\mathrm{I}(\mathbf{x}, \omega)$ can be generalized to a variable rupture speed by replacing the linear time delay ξ_1/v in the integrand of equation (4) by a spatially variable delay $\Delta t(\xi_1)$ of arbitrary form:

$$\mathrm{I}(\mathbf{x}, \omega) = \int_0^L \exp\left\{ i\omega \left[\Delta t(\xi_1) - \frac{\xi_1 \cos \Psi}{c} \right] \right\} d\xi_1. \tag{6}$$

The integral (equation 6) can then be evaluated numerically. The subsequent example was produced for a fault with the length $L = 3400$ m, corresponding to an M_w 5 earthquake according to the empirical relationship between fault area and moment magnitude of Wells and Coppersmith (1994, their table 2A). The rupture velocity v was randomized to

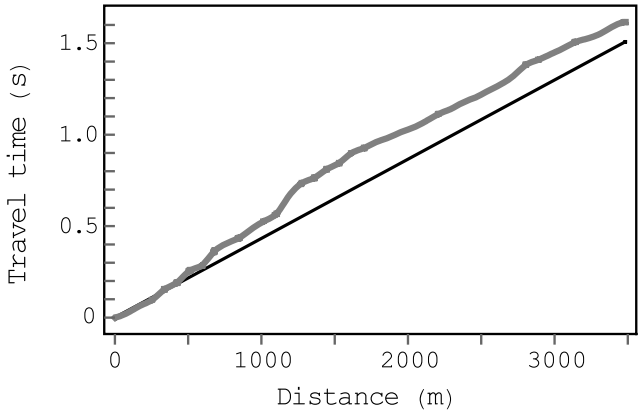

Figure 1. Rupture-propagation times along the fault for the constant and randomized velocities.

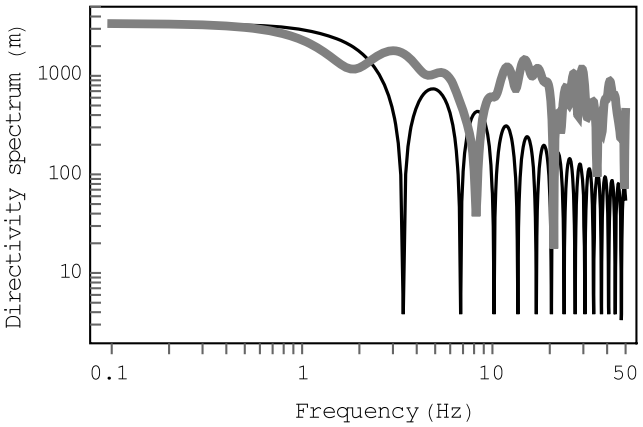

Figure 2. Moduli of the finite-fault directivity spectra for the cases of constant and randomly perturbed rupture velocities (black and gray lines, respectively).

result in a spatially variable propagation time as follows. The fault length was divided into 40 equal intervals with the length ΔL, and the incremental rupture travel time through each consecutive ith segment was calculated as $\Delta t_i = \Delta L/[v(1+\eta)]$. The random variable η for each segment was drawn form a normal distribution with zero mean and standard deviation of 0.3, constrained to equal -0.9 if its value accidentally fell below or was equal to -1. The value of v was chosen as 0.8β, in which β is the S-wave velocity, which in turn was chosen as $5000/\sqrt{3}$ m/s. The resulting grid of 40 travel-time values was interpolated to produce a smooth perturbed curve $\Delta t(\xi_1)$. Both the constant- and randomized velocity travel-time curves are shown in Figure 1.

Figure 2 compares the directivity spectra $|\mathbf{I}(\mathbf{x},\omega)|$ of a radiated shear wave ($c = \beta$) for the cases of constant and randomized rupture speeds and $\Psi = 0$ (radiation in the direction of rupture propagation). The former case (black line) was calculated from equation (5) and the latter (gray line) computed by the numerical evaluation of integral (equation 6) with the interpolated function $\Delta t(\xi_1)$ in the integrand, generated as explained.

As pointed out, the constant-speed spectrum (black line) in Figure 2 is the sinc function with the envelope falling off as ω^{-1}. However, the high-frequency spectrum for the randomized velocity is nearly flat. As a result, the radiated spectrum (equation 3) is controlled by that of the source time function and is almost unaffected by the source finiteness. The steeper high-frequency fall-off in the former case is an artifact caused by the assumption of constant v, which produces a regular pattern of destructive interference with the shape of a sinc function (Aki and Richards, 1980, p. 810). Randomness in the timing of rupture at different parts of the fault suppresses the regular interference, nearly eliminating the additional slope. The spectrum of radiation from the finite source becomes nearly identical to that of the source time function.

The condition of constant rupture velocity is an idealization that admittedly never materializes in reality, eliminating the possibility of a steeper slope induced by the regular interference. In the general case, free of the limiting assumptions leading to equations (3) and (4), the finite-fault radiation is described by equation (2). The latter shows that the effects of the finite source size will modulate the underlying slip-function spectrum $\Delta u(\omega)$ albeit most probably in an irregular and unpredictable manner. The average dominance of the underlying spectrum over the fault directivity in controlling the seismic radiation (Beresnev, 2017) should thus be recognized not just as a point-source effect but as a more general phenomenon.

Frankel (2019) argues that the ω^{-2} spectral fall-off in the source term of the displacement spectra radiated into the far field (known as the omega-square model) is widely recognized. This contradicts our own experience. In the study by Anil-Bayrak and Beresnev (2009), we specifically looked for the omega-square seismic spectra to resolve the fault-slip velocities from their corner frequencies. A large database of all earthquake records of the KiK-net network in Japan available to date was scanned for the spectra following the model. The search was conducted for all events in the magnitude range from 4 to 6 recorded by at least two rock sites. Only five earthquakes with the required fall-off were found: the spectra of all others exhibited deviations that could not be strictly fit with the omega-square assumption. Uchide and Imanishi (2016) report similar results.

References

Aki, K., and P. G. Richards (1980). *Quantitative Seismology*, W. H. Freeman and Company, San Francisco, California.

Anil-Bayrak, N. A., and I. A. Beresnev (2009). Fault slip velocities inferred from the spectra of ground motions, *Bull. Seismol. Soc. Am.* **99,** 876–883.

Beresnev, I. A. (2017). Factors controlling high-frequency radiation from extended ruptures, *J. Seismol.* **21,** 1277–1284.

Beresnev, I. A. (2019). Interpretation of kappa and $f_{\max}$ filters as source effect, *Bull. Seismol. Soc. Am.* **109,** 822–826.

Frankel, A. (2019). "Comment on" Interpretation of kappa and f_{max} filters as source effect" by Igor A. Beresnev", *Bull. Seismol. Soc. Am.* doi: 10.1785/0120190085.

Uchide, T., and K. Imanishi (2016). Small earthquakes deviate from the omega-square model as revealed by multiple spectral ratio analysis, *Bull. Seismol. Soc. Am.* **106,** 1357–1363.

Wells, D. L., and K. J. Coppersmith (1994). New empirical relationships among magnitude, rupture length, rupture width, rupture area, and surface displacement, *Bull. Seismol. Soc. Am.* **84,** 974–1002.

Department of Geological and Atmospheric Sciences
Iowa State University
253 Science I, 2237 Osborn Drive
Ames, Iowa 50011-3212 U.S.A.
beresnev@iastate.edu

Manuscript received 15 May 2019;
Published Online 12 November 2019